

Electron velocity distribution functions in a sputtering magnetron discharge for the $\mathbf{E} \times \mathbf{B}$ direction

T. E. Sheridan,^{a)} M. J. Goeckner,^{b)} and J. Goree

Department of Physics and Astronomy, The University of Iowa, Iowa City, Iowa 52242

(Received 24 October 1997; accepted 20 February 1998)

The electron velocity distribution function is measured for the $\mathbf{E} \times \mathbf{B}$ (azimuthal) direction in a cylindrically symmetric, planar, sputtering magnetron discharge as a function of height above the cathode. Near the cathode, the distribution function is approximately a warm Maxwellian ($T_e \approx 2$ eV) shifted in the $\mathbf{E} \times \mathbf{B}$ direction, indicating a strong azimuthal drift. Farther above the cathode, the distribution function is characterized by a cold ($T_e \approx 0.5$ eV), Maxwellian bulk with energetic, asymmetric tails. © 1998 American Vacuum Society. [S0734-2101(98)05304-4]

I. INTRODUCTION

In a magnetron discharge, crossed electric and magnetic fields, \mathbf{E} and \mathbf{B} , respectively, confine electrons in closed $\mathbf{E} \times \mathbf{B}$ drift loops near a negatively biased cathode target.^{1,2} Here, \mathbf{E} is provided by the plasma sheath and presheath while \mathbf{B} is produced either by permanent magnets or current-carrying coils. The confined electrons ionize neutral gas atoms, creating a region of intense ionization adjacent to the cathode. Ions born in the electron trap region are then accelerated by the plasma sheath to the cathode target (ions are essentially unmagnetized), and impact there with several hundred electron volts of energy, sputtering atoms from the target and causing secondary electron emission. The secondary electrons are accelerated back into the magnetic trap region, helping to sustain the discharge.²

The presence of an electron $\mathbf{E} \times \mathbf{B}$ drift has been inferred experimentally in several ways: through the difference in current collected by one-sided Langmuir probes,³ by changes in the magnetic field above the discharge,⁴ and from the distortion of cylindrical probe characteristics.⁵ An azimuthal electron drift has also been observed in Monte Carlo simulations of electron orbits.² Though these observations confirm that an $\mathbf{E} \times \mathbf{B}$ drift is present, they suffer from the deficiencies that they are indirect, and that they do not provide details about the electron distribution function.

In this article, we use a one-sided, planar Langmuir probe⁶ to directly measure the electron velocity distribution function in the $\mathbf{E} \times \mathbf{B}$ (azimuthal) direction in a cylindrically symmetric, planar magnetron. We find a strong electron drift near the top of the magnetic trap, while outside the trap the distribution function is seen to have cold Maxwellian and energetic tail components. In Sec. II, the magnetron and diagnostics are described, and results are presented and discussed in Sec. III. Conclusions are given in Sec. IV.

II. APPARATUS

Measurements were made for a cylindrically symmetric, planar magnetron (76.2-mm-diam cathode) that has been described elsewhere.⁷ The magnetic field [Fig. 1(a)] is dominated by the dipole moment of an outer magnetic ring, so that field lines above the magnetic trap region are predominantly in the axial direction. This magnetic configuration is classified as a type II unbalanced magnetron,⁸ so that the dominant electron losses are axial rather than radial. The magnetic field in this device is tangential to the cathode at a radius $r = 17$ mm [$B_r = 245$ G, Fig. 1(b)], and this is where the etch track is deepest.

For the measurements reported here, we use a one-sided planar Langmuir probe⁶ (3.4-mm-diam) to deduce the reduced electron velocity distribution function $g(v_\theta)$ in the azimuthal direction. At any point in space the electron distribution function f depends on three orthogonal velocity components, i.e., $f = f(v_r, v_\theta, v_z)$, where (r, θ, z) represents three locally orthogonal directions rather than a global coordinate system. Using a planar probe we measure the current-voltage characteristic in the azimuthal direction (i.e., θ) and thereby determine the v_θ dependence of the distribution function. In other words, $f(v_r, v_\theta, v_z)$ is reduced to $g(v_\theta)$ by integrating over the two directions orthogonal to the probe face, i.e., r and z , giving

$$g(v_\theta) = \int_{-\infty}^{\infty} dv_r \int_{-\infty}^{\infty} dv_z f(v_r, v_\theta, v_z). \quad (1)$$

The positive- and negative-velocity halves of $g(v_\theta)$ are found by measuring the current-voltage characteristic in antiparallel directions, where $g(v_\theta)$ is recovered from the first derivative of the probe characteristics (for more details see Ref. 6).

The “first derivative” method outlined above makes fewer assumptions about the distribution function than other analysis techniques. For example, in the most common procedure a distribution function is assumed (usually, a stationary Maxwellian) and plasma parameters are found by fitting a predicted characteristic to the probe data.⁵ While, if the “second derivative” method is used to measure the electron energy distribution function, isotropy is assumed. Such as-

^{a)}Present address: Space Plasma and Plasma Processing Group, Plasma Research Laboratory, Research School of Physical Sciences and Engineering, Australian National University, Canberra, Australian Capital Territory 0200, Australia. Electronic mail: terry.sheridan@anu.edu.au

^{b)}Present address: Princeton Plasma Physics Laboratory, P.O. Box 451, Princeton, New Jersey 08543.

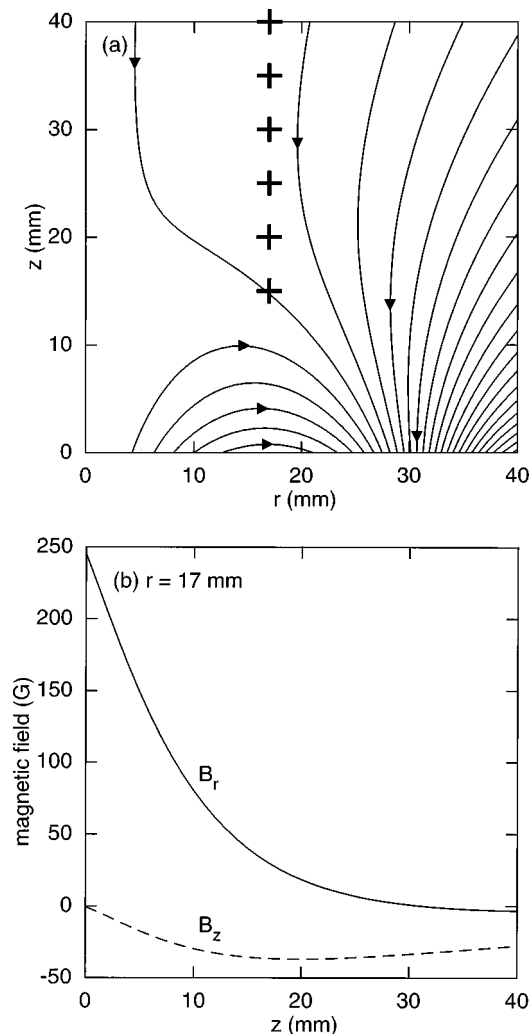


FIG. 1. (a) Magnetic-field configuration in the r - z plane and (b) z dependence of magnetic-field components B_r and B_z for $r=17$ mm. The magnetron is a cylindrically symmetric, planar device with the cathode at $z=0$. Crosses in (a) mark the locations where the azimuthal electron distribution function is measured.

assumptions make sense at high pressures where the electron mean-free path is short. However, they are not justified in low-pressure, anisotropic discharges such as the sputtering magnetron.

Once the reduced distribution function $g(v_\theta)$ has been determined, moments can be computed:⁶ including the electron density n_e , the azimuthal drift velocity $\langle v_\theta \rangle$, and the average electron energy, $1/2m\langle v_\theta^2 \rangle$. The azimuthal current density is $J_\theta = en_e\langle v_\theta \rangle$. When the distribution function is non-Maxwellian, as will be the case here, the average random energy can be related to an "effective temperature" by $T_{\text{eff}} = m\langle (v_\theta - \langle v_\theta \rangle)^2 \rangle/k$.

III. RESULTS

A copper cathode was used with Ar gas at a pressure of 1.0 Pa. The discharge voltage was -400 V dc, and the discharge current was 51 mA, giving a current density at the cathode of ≈ 46 A/m². Measurements were made in the azi-

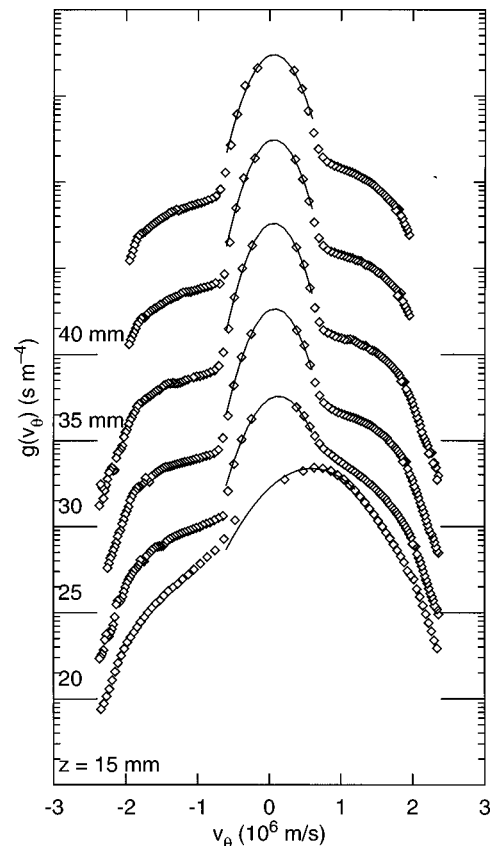


FIG. 2. Reduced electron velocity distribution functions $g(v_\theta)$ at $r=17$ mm for heights $z=15, 20, 25, 30, 35,$ and 40 mm above the cathode. The abscissa is logarithmic. Each distribution function begins at 10^6 s m⁻⁴ at the position indicated on the g axis. An $\mathbf{E} \times \mathbf{B}$ drift is clearly seen at $z=15$ mm.

muthal direction at a radius $r=17$ mm (above the deepest part of the etch track) and for six heights above the cathode $z=15, 20, 25, 30, 35,$ and 40 mm, as shown in Fig. 1(a). Unfortunately, it was not possible to make measurements nearer the cathode, as the presence of the probe caused a large decrease in the discharge current. (This observation agrees qualitatively with Monte Carlo simulations² showing that the trap region extends ≈ 10 mm above the cathode.) Note in Fig. 1 that $r=17$ mm, $z=15$ mm is almost on the magnetic "separatrix," i.e., for $z \leq 15$ mm, magnetic-field lines begin and end on the cathode, giving a rough indication of the trap region, while for $z \geq 15$ mm, magnetic-field lines connect the cathode to the anode, allowing energetic electrons to escape axially.⁶

The measured electron velocity distribution functions $g(v_\theta)$ are shown in Fig. 2, where positive velocities are in the $\mathbf{E} \times \mathbf{B}$ drift direction and the vertical axis is logarithmic to bring out detail in the tails. A shifted-Maxwellian curve is used to interpolate the distribution function⁶ around $v_\theta=0$.

The most striking feature of the distribution function nearest the cathode ($z=15$ mm) is a clear drift in the $\mathbf{E} \times \mathbf{B}$ direction. Here, the distribution function consists of a warm Maxwellian ($T \approx 1.9$ eV) shifted in the positive direction by the $\mathbf{E} \times \mathbf{B}$ drift. The distribution function is asymmetric about

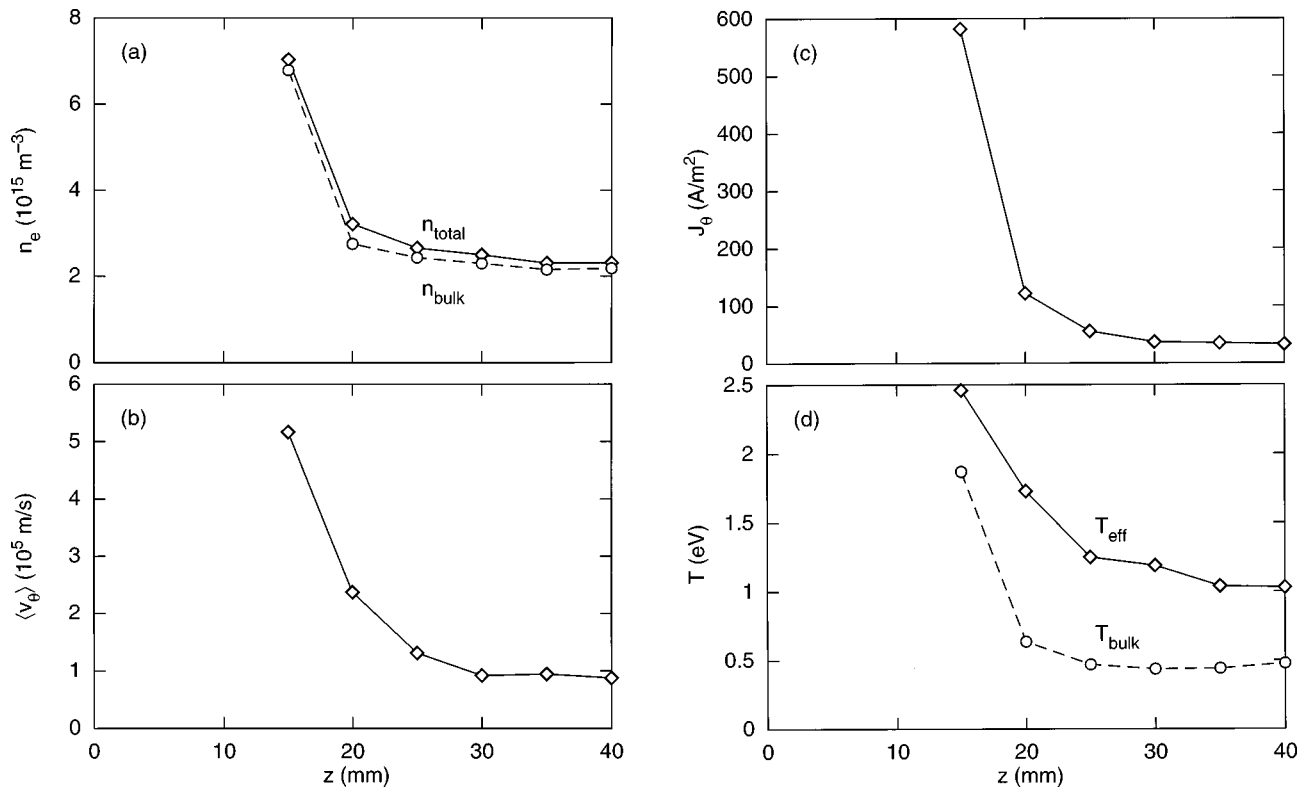


FIG. 3. Axial dependence of the (a) electron density n_e , (b) average azimuthal velocity $\langle v_\theta \rangle$, (c) azimuthal current density J_θ , and (d) the electron temperature. Here, n_{total} is the total electron density computed by integrating $g(v_\theta)$, n_{bulk} is the density of the fitted Maxwellian component, T_{eff} is the effective temperature found from the second moment of the distribution function, and T_{bulk} is the temperature of the fitted Maxwellian.

its peak, with a small tail in the negative-velocity direction that may be due to backscattered electrons. The drift velocity of the distribution found from fitting the shifted Maxwellian is 6.0×10^5 m/s, while that found by integrated g is $\langle v_\theta \rangle = 5.2 \times 10^5$ m/s, which is slightly smaller due to the negative-velocity tail. If we assume that \mathbf{E} is in the z direction, then the magnitude of the $\mathbf{E} \times \mathbf{B}$ drift in the θ direction is E_z/B_r , where $B_r \approx 0.0040$ T [Fig. 1(b)] implying $E_z \approx 24$ V/cm. For comparison, using a cylindrical probe⁵ at $r = 19$ mm and $z = 13$ mm and for a lesser pressure of 0.42 Pa, a drift velocity of 1.34×10^6 m/s was inferred, indicating that the drift velocity may increase as the pressure decreases. Such an increase has also been inferred⁴ from changes in the magnetic field above the cathode, and would seem to indicate that the electric field increases (i.e., the sheath grows) as the pressure decreases.

For $z \geq 20$ mm, $g(v_\theta)$ consists of a cold, stationary Maxwellian ($T \approx 0.5$ eV) with nearly rectangular tails (Fig. 2). Here, the cold population most likely consists of electrons trapped in the “axial” plasma potential well, as has previously been seen for measurements in the z direction.⁶ The distribution function falls off rapidly above $|v_\theta| \approx 2 \times 10^6$ m/s due to the removal of high-energy electrons above the inelastic threshold⁹ for Ar (11.55 eV or 2.04×10^6 m/s). Rectangular tails such as those seen here are consistent with approximately monoenergetic electrons having an isotropic velocity distribution after “reduction” using Eq. (1).^{10,11} It may be that these electrons are scattered elastically out of the

main axial flow⁶—the scattering cross section in Ar is largest at ≈ 10 eV, while the electron distribution function is cutoff above the inelastic threshold so that electrons with energies just below that threshold should be scattered preferentially. The shoulder on the $\mathbf{E} \times \mathbf{B}$ side of the distribution is always higher than that on the opposing side, giving a small residual $\mathbf{E} \times \mathbf{B}$ drift. For larger values of z the asymmetry seen in the tails of the distribution may be due to energetic electrons scattered out of the trap since elastic scattering is predominantly forward.

Both the total and bulk electron densities decrease sharply outside the trap region, and become nearly constant for $z \geq 20$ mm as shown in Fig. 3(a). Here, the bulk density is found from the fitted Maxwellian (i.e., without the tails), while the total density is found by integrating g . The total density is only slightly greater than the bulk density, as the fraction of tail electrons is quite small. The value of n_e found at $z = 25$ mm is in good agreement with that calculated⁶ from the *axial* reduced distribution function $g(v_z)$ at the nearby position $r = 15$ mm, $z = 25$ mm, indicating that the measurement is internally consistent. (The total density should be the same irrespective of the direction for which g is measured.)

The average azimuthal drift velocity [Fig. 3(b)] is largest near the cathode, due to the strong asymmetry in g —only for $z = 15$ mm is the peak of the fitted Maxwellian shifted appreciably from zero. For $z \geq 20$ mm, the small drift velocity is due to the asymmetry of the tails, rather than to a shift of the bulk.

The azimuthal current density J_θ [Fig. 3(c)] is the product of the electron density and the azimuthal drift velocity, and so is quite large nearest the cathode since both the electron density and the drift velocity are greatest there. The azimuthal current density then decays rapidly with z as both the density and drift velocity decrease outside of the magnetic trap region and J_θ becomes approximately constant far above the cathode. For $z = 15$ mm, J_θ is ≈ 10 times larger than the average current density to the cathode, while farther from the cathode the two quantities are comparable.

The effective electron "temperature" T_{eff} is computed from the second moment of g and is, therefore, sensitive to the tails of the distribution, while the bulk temperature T_{bulk} is found from the fitted Maxwellian. (Previously,¹² two electron temperatures were observed using a cylindrical Langmuir probe.) Hence, T_{eff} decreases rapidly just above the magnetic trap, and then becomes nearly constant for $z \geq 25$ mm, as shown in Fig. 3(d). The bulk electron temperature determined from the fitted Maxwellian has an approximately constant value of 0.5 eV above the trap, while only the point nearest the trap has a much higher temperature.

IV. CONCLUSIONS

We have found that the electron velocity distribution function in the azimuthal direction in a low-pressure magnetron discharge is neither Maxwellian nor isotropic. Near the magnetic trap, the distribution function is approximately a warm Maxwellian drifting in the $\mathbf{E} \times \mathbf{B}$ direction, while farther above the trap we find a cold Maxwellian bulk with asymmetric rectangular tails. These measurements provide direct evidence for the $\mathbf{E} \times \mathbf{B}$ electron drift as well as detailed information about the morphology of the distribution function in the azimuthal direction.

These results also have implications for the interpretation of cylindrical Langmuir probe characteristics. In particular, the probe characteristics for a drifting distribution function

may be misinterpreted as a stationary distribution with an erroneously high electron temperature.⁵ It has previously been reported that the electron temperature increases as pressure decreases,¹³ approaching values as high as 20 eV in the trap region. However, at least part of this apparent increase in temperature may be due to an increasing drift velocity.

Finally, the $\mathbf{E} \times \mathbf{B}$ electron drift increases the ionization rate above that due to a stationary Maxwellian of the same temperature by raising the average electron energy, especially closer to the cathode, where both the electric and magnetic fields are larger. This effect may contribute significantly to the overall ionization rate in certain regimes.

ACKNOWLEDGMENTS

This work was supported by the Iowa Department of Economic Development and the National Science Foundation. The authors would like to thank M. A. Lieberman for useful comments.

¹A. E. Wendt, M. A. Lieberman, and H. Meuth, *J. Vac. Sci. Technol. A* **6**, 1827 (1988).

²T. E. Sheridan, M. J. Goeckner, and J. Goree, *J. Vac. Sci. Technol. A* **8**, 30 (1990).

³H. Fujita, S. Yagura, H. Ueno, and M. Nagano, *J. Phys. D* **19**, 1699 (1986).

⁴S. M. Rossnagel and H. R. Kaufman, *J. Vac. Sci. Technol. A* **5**, 88 (1987).

⁵T. E. Sheridan and J. Goree, *Phys. Rev. E* **50**, 2991 (1994).

⁶T. E. Sheridan, M. J. Goeckner, and J. Goree, *Jpn. J. Appl. Phys., Part 1* **34**, 4977 (1995).

⁷T. E. Sheridan and J. Goree, *J. Vac. Sci. Technol. A* **7**, 1014 (1989).

⁸B. Windows and N. Savvides, *J. Vac. Sci. Technol. A* **4**, 196 (1986).

⁹J. L. Blank, *Phys. Fluids* **11**, 1686 (1968).

¹⁰N. Hershkowitz, J. R. DeKock, P. Coakley, and S. L. Cartier, *Rev. Sci. Instrum.* **51**, 64 (1980).

¹¹N. Hershkowitz, R. L. Goettsch, C. Chan, K. Hendriks, and R. T. Carpenter, *J. Appl. Phys.* **53**, 5330 (1982).

¹²T. E. Sheridan, M. J. Goeckner, and J. Goree, *J. Vac. Sci. Technol. A* **9**, 688 (1991).

¹³S. M. Rossnagel and H. R. Kaufman, *J. Vac. Sci. Technol. A* **4**, 1822 (1986).